RSC Advances

ROYAL SOCIETY OF CHEMISTRY

www.rsc.org/advances

Journal Name

ARTICLE

Thermal reduction to control the spacing in graphene oxide membranes: Effect on ion diffusion and electrical conduction

Received 00th January 20xx,
Accepted 00th January 20xx

DOI: 10.1039/x0xx00000x

www.rsc.org/

A. Alhadhrami,[a] S. Salgado[a] and V. Maheshwari[c]

Means to control the inter-layer spacing in graphene oxide and reduced graphene oxide membranes is required to tailor their properties. We report that based on the temperature of thermal reduction the interlayer spacing in these membranes can be controlled from 7.6 °A to 4.6 °A. This is the critic al range that matches with the hydrated ionic radii of commonly found ions in water and hence is useful to tailor the diffusion characteristics of these membranes. In accordance with the change in inter layer spacing, both the in-plane and out of plane electrical conductivity of the membranes also increases and this is also observed in the electrochemical characteristic of the membranes.

Introduction

Graphene, graphene oxide (GO) and reduced graphene oxide (rGO) membranes (or films) are being actively researched for their diffusion characteristics[1-8] and also as electrochemical electrodes.[9-16] The research is driven by the potential of using these membranes for desalination, water purification, and gas separation,[1-5] as supercapacitors[9;14;17-20] and electrochemical devices,[5;8;10;12;13;15;16] and in a broader sense to control the diffusion and interaction of ions and molecules with them. Two kinds of GO and rGO membranes have been of primary interest, one consisting of a single sheet and other where a multilayer stack of sheets is assembled into a membrane. A defect free single graphene sheet is impermeable to ionic species in aqueous medium.[21;22] In case of multilayer membranes which consist of stack of overlapping GO (or rGO) sheets, the inter-layer spacing between the sheets is the critical factor that affects the diffusion of the ionic species.[1;3;5;7] Typically if the inter-layer spacing is large enough then ionic species can easily diffuse across the membrane. The control over the inter-sheet spacing is hence a crucial parameter for modulating the diffusion characteristics of the graphene membranes. Similarly, interlayer spacing in the GO and rGO membranes also affects their porous structure and is therefore also critical for their application as supercapacitors and as a working electrode in electrochemical sensors.[23-25] The mechanical properties of these films as graphene paper is also an active area of research due to their varied range of applications and is affected by these parameters.[26-29] Further the use of GO and its derivatives as fillers in polymer matrix which leads to enhanced properties is also affected by the interlayer interaction between the GO sheets as it critically affecting the mechanical and electrical properties of the composite.[30-34] Here we report that membranes made with GO have a large inter-layer spacing due to the functional groups present on its surface. The interlayer spacing can be modulated by reduction of these membranes. This is accomplished by a simple ambient thermal reduction[35] which causes the removal of the functional groups and therefore decreases the inter-layer spacing from 7.6 °A to 4.6 °A. The extent of reduction and the change in the interlayer spacing of the membranes is dependent on the temperature at which thermal reduction is performed. Corresponding to the removal of the functional groups (or defects) the change in the interlayer spacing is also reflected in both the in-plane and out-of-plane electrical conductivity of these membranes. This change also critically affects the mechanical properties of these films due to reduced chemical interaction between the adjacent layers. Following this, our results also show that the diffusion characteristics of these membranes reflect the changes in their interlayer spacing and this can be tuned based on the temperature used for thermal reduction.

An aqueous suspension of graphene oxide sheets is synthesized by the chemical oxidation and exfoliation route (modified Hummer's method).[36;37] Following this, graphene sheets are assembled into membranes by vacuum filtration.[38;39] The resulting membranes basically consist of stacks of GO sheets across their vertical cross-section. Considering the in-plane morphology of the membranes, GO sheets form an overlaying patchwork. The thickness of the membrane is controlled by the volume of the GO solution filtered. This method has been used to make large area transparent films of GO for use as electrodes in supercapacitors and electrochemical sensors, after their

[a] A.A., S.S., V.M.
Dept. of Chemistry, Waterloo Institute of Nanotechnology, University of Waterloo 200 University Ave. West, Waterloo ON N2G 3L1, Canada
E-mail: vmaheshw@uwaterloo.ca

Information (ESI) available: [details of any supplementary information available should be included here]. See DOI: 10.1039/x0xx00000x

reduction.[39] It has also been used to make large area GO membranes which have been studied for their ion diffusion characteristic and reported to have selective ion diffusion rates based on the charge and size of the ions. The diffusion rate and the selectivity across these membranes is dependent on two critical parameters namely, the functional groups on the GO sheets and the interlayer spacing that determines the available free volume for the ions to diffuse.[7] This also determines the porosity of such a GO membrane and affects its electrochemical performance.[23;24;40] Both these parameters are dependent on the level of oxidation of the graphene sheets.[24;41] The primary functional groups, carboxylic, hydroxyl and epoxy, cause both an increase in the interlayer spacing when the GO sheets are assembled as membranes and also interact with the ions, primarily the cations, and affect their ability to diffuse across the membrane. The dual ability of these functional groups can hence be used to tailor the diffusion properties of the GO membranes. We demonstrate this by thermally reducing the GO (TrGO) sheets to vary the density of these functional groups and directly modulate their diffusional characteristics.

Experimental

GO is synthesized via the modified Hummer's method. GO membranes are made via vacuum filtration through anodisc filters (25 mm in diameter, 0.02 µm pore size). These GO membranes are then exposed in an oven to the appropriate temperature for thermal reduction. Both vertical and horizontal electrical conductivity tests on the TrGO membranes are performed by making silver contacts. Diffusion characteristics of the TrGO membranes were tested in a home build set-up (details in ESI).

Results and Discussion

GO made by modified Hummer's method is assembled into membranes by vacuum filtration.[7;36;37;39] A typical membrane as shown in the field emission microscopy (FESEM) image of Figure 1a consists of stacked GO sheets. The inset shows the top view of the membrane. To illustrate the spacing between the GO sheets and its periodicity, X-ray diffraction (XRD) is performed on the membrane. As seen in Figure 1b we see a strong peak at 2θ ~ 12°, which corresponds to an inter-layer spacing of 7.4 ºA for the membrane dried at 60 °C. The effect of thermal reduction is illustrated by exposing the GO membrane for 30 minutes to six different temperatures in air, 60ºC, 180 ºC, 200 ºC, 225 ºC, 250 ºC and 300 ºC. As a result of this exposure we can see in the XRD data of Figure 1c that the peak corresponding to the interlayer spacing shifts to larger angles, signifying the reduction in the spacing. As seen in Figure 1d we observe a gradual change in the spacing in going from 60 ºC to 180 ºC and 200 ºC. It decreases from 7.4 ºA to 6.9 ºA to 6.5 ºA, respectively. Further increasing the reduction temperature to 225ºC decreases the spacing to 4.8 ºA. Following this, little change is observed on increasing the temperature to 250 ºC or 300 ºC, spacing of 4.6 ºA and 4.57 ºA respectively. A broadening of the peak is observed with reduction leading to the conclusion that the order in interlayer spacing also decreases. The change in inter-layer spacing with thermal treatment is collaborated by thermal gravimetric analysis (TGA). Three transitions that lead to weight loss are observed (Figure 1e). At ~ 60 ºC -100 ºC the loss in weight is associated with the thermal removal of residual water molecules in the GO membrane. Following this the weight is relatively constant till ~ 200 ºC, when a further reduction in mass of the GO membrane is observed.[35] This corresponds to the sharp transition observed in the XRD data due to the reduction of the inter-layer spacing in the GO membrane. The combined TGA and XRD data lead to conclusion that the change from 60 ºC to 180 ºC corresponds primarily to the evaporation of water molecules in these hygroscopic films. A further increase in temperature to 225ºC causes the removal of the surface groups (defects) caused by the oxidative treatment of the graphite during exfoliation to form GO sheets and physisorbed water on the GO sheets. Increasing the temperature further only causes a minimal change in the spacing, leading to the conclusion defects are primarily removed by 225ºC.[42;43] Finally at ~ 550 ºC complete degradation of the membrane reduces the weight to ~0. These transitions can be more clearly observed in Figure 1f, where the rate of weight change with temperature for the membrane is plotted. Results from FTIR studies presented below further corroborate these observations (details in ESI).

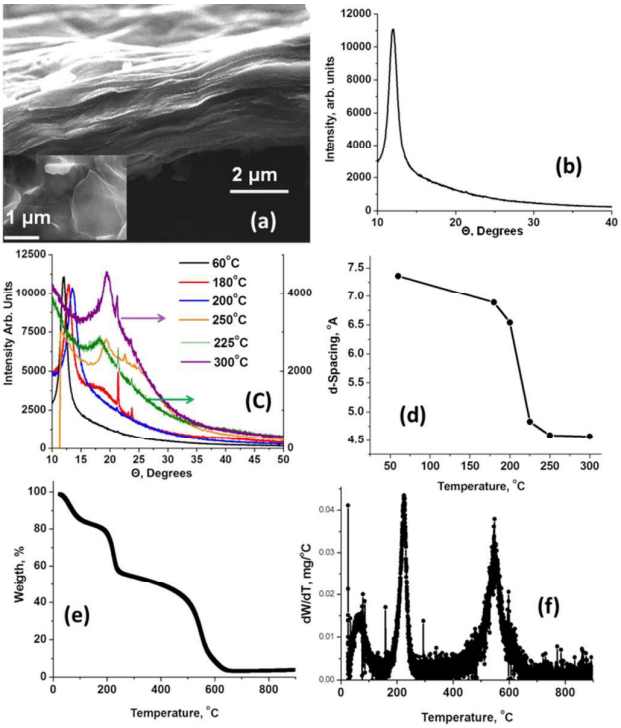

Figure 1. (a) FESEM image showing the stacked GO sheets in a membrane. The inset is the top view that shows overlapping GO sheets. (b) The XRD pattern of a GO sheet dried at 60°C shows a sharp peak corresponding to an interlayer spacing of 7.4 °A. (c) On thermal reduction the XRD spectrum shows that the spacing decreases with increasing temperature of processing. (d) The spacing as

calculated from the peak positon shows that the spacing decreases from ~ 7.4 °A to ~ 4.6 °A due to the thermal reduction with increasing temperature. (e) The TGA analysis of the GO membrane shows the effect of temperature on the weight transitions with three loss regions being observed. (f) A plot of the derivative of the TGA curve more specifically shows the peak loss temperature regions being ~ 100°C, 200°C and 550°C

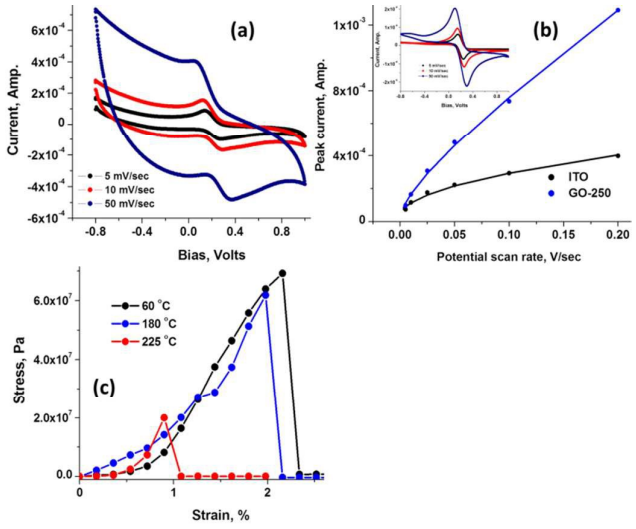

Figure 2. The electrochemical and mechanical performance of TrGO films. (a)&(b) CV plots for films reduced at 250°C in $K_3Fe(CN)_6$. (a) The potential scans at different scan rates show the characteristic redox peaks. The constant current background due to capacitive nature of the TrGO films is clearly visible. (b) The peak reduction current for both TrGO and ITO fits to to $Cυ + Kυ^{0.5}$. The inset shows potential scan on ITO substrate, the background capacitive currents are greatly diminished compared to TrGO films. (c) The response of TrGO films reduced at 60 °C, 180 °C and 250 °C in tensile testing.

The Raman analysis of the GO and Tr-GO membranes shows that similar to reduction of GO with chemicals such as hydrazine and ascorbic acid, an increase in I_D/I_G (the relative intensity of the D band at ~1350 cm^{-1} and G band at 1590 cm^{-1}) is observed. The ratio increases from 0.85 at 60 ºC to ~ 0.95 at 225 ºC (see ESI, Fig. S1).[35;44;45] The FT-IR data also shows the effects of reduction. The absorption bands at 1060 cm^{-1} (epoxy and alkoxy), 2300-2400 cm^{-1} (C≡C or C≡N) and 3400 cm^{-1} (a very broad peak due to O-H), decrease gradually in intensity with thermal reduction (details in ESI Fig. S1).[35;42;46;47] While the absorption peak of C=C at 1600 cm^{-1} (due to sp2 hybridized carbon) is not affected by the thermal treatment. The presence of nitrogen can be the result of impurities in the chemicals used during the oxidation process to form GO. However, not all functional groups are removed by reduction with the thermal treatment, in line with other reduction methods which also partially restore the sp2 framework of GO (details in ESI). X-ray photoelectron spectroscopy (XPS) analysis of the Tr-GO and GO films for the C1S region further supports this analysis. The ratio of C-C (non-oxygenated ring carbon) to that of C-O & O-C=O (oxygenated carbon) is ~ 1.09 for Tr-GO films processed at 60 ºC, this increases slight to 1.122 for films processed at 180 ºC, but increases substantially for the Tr-GO films reduced at 250 ºC to 3.85 (details in ESI).[48]

The effect of thermal reduction on the electrochemical performance of the GO films is illustrated by using them as electrodes for the redox of $K_3Fe(CN)_6$ in cyclic voltammetry scans (CV). Films treated at 60 ºC and 180 ºC do not show a discernible redox peak for $K_3Fe(CN)_6$ (in linear cyclic potential sweeps) and the current is orders of magnitude lower (details in ESI). This is due to the high intrinsic resistance of these films which leads to a large ohmic drop in their structure.[24;49;50] In comparison films reduced at 250 ºC show a prominent $K_3Fe(CN)_6$ redox peak with current levels in the range of 10^{-4}-10^{-3} amp/cm^2, Figure 2a. The intensity of the redox currents for the 250 ºC film is comparable to that of ITO (inset of Figure 2b). The large background current (in rectangular shape) is manifestation of the capacitive nature of the Tr-GO film due to the formation of electrical double layer.[9;14;19] Further we see from Figure 2b that the peak current can be fit as being proportional to $Cυ + Kυ^{0.5}$ (υ is the potential scan rate). The first term is due to the capacitance of the film and the second term is the dependence of the redox current on scan rate for a typical electrode. Identical experiments are performed with ITO (Indium Tin Oxide coated glass slide), inset of Figure 2b. The comparison of C (the capacitance) and K (the redox parameter for the electrode and the specie) shows that for the Tr-GO film 'C' ($3x10^{-3}$ F/cm^2) is more than two orders of magnitude higher than that of ITO ($1x10^{-5}$ F/cm^2), while 'K' is more comparable ($1.21x10^{-3}$ (amp/cm^2).(Sec/V)$^{1/2}$ for Tr-GO and $8.3x10^{-4}$ (amp/cm^2).(Sec/V)$^{1/2}$for ITO). The comparable values of K signify that the ITO and Tr-GO film have very similar redox performance as substrates.[23;40] However, the significantly higher capacitive nature of the film is indicative of pseudo capacitance due to residual functional groups and the porous nature of these films due to interlayer spacing.[51-55] Further the films electrochemical performance illustrates that despite thermal reduction and the partial removal of the functional groups, aqueous ions can still easily access its surface.[56] The access is also required to enable the functioning of these films as membranes in aqueous medium.

The mechanical characteristic of these films is illustrated in Figure 2c. The Tr-GO films processed at 60°C and 180°C have similar behaviour with a failure stress of 69.7 MPa and 61.8 MPa.[26;27] For the Tr-GO film processed at 225°C this reduces significantly to 20 MPa. This is consistent as the presence of oxygen functional groups and water molecules between adjacent layers will improve the interlayer forces due to hydrogen bonding and also interlayer interaction between the functional groups.[27;28] The high failure strains are the result of wrinkles in these films.[29] The mechanical and electrical characteristics of Tr-GO are critical for their use as nano fillers in polymer composites with improved thermal stability and electrical properties.[30-32]

Compared to Graphene sheets,[57;58] GO is an electrical insulator due to the high density of functional groups.[37;39;49]

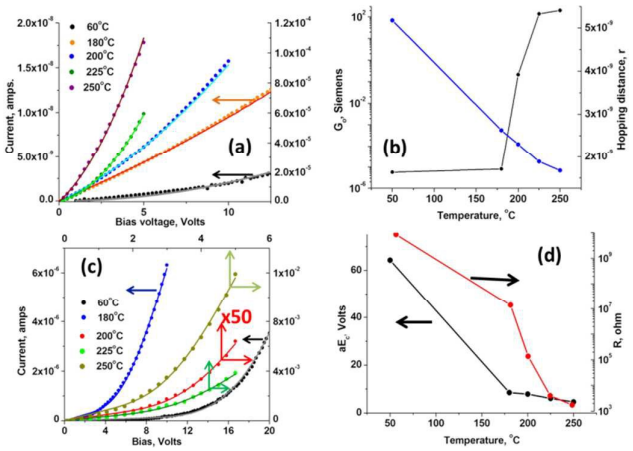

Figure 3. Effect of thermal reduction on electrical conductivity of the membranes. (a) Horizontal conduction measured over a distance of 5mm. The data points are actual measurement values and the line is the fit from the charge hopping model as shown in eq. 1. A significant increase in conductivity is observed when the temperature of reduction is above 180 °C. (b) From the fit the change in the parameters of the hopping model, Go and r, the hopping distance with temperature is observed. As expected r decreases with temperature of reduction and Go increases. (c) Vertical conduction measurement over the TrGO membranes. The data points are experimental values and the line is the fit from eq. 2. Again we observe an increase in conductance with increasing temperature. A similar sharp increase in conductivity is observed above 180 °C. (d) The parameters aE_c and R evolve with temperature and in line with decreasing interlayer spacing. Both aE_c and R decrease significantly with temperature.

As GO is reduced, the removal of the functional groups leads to an increase in the electrical conductivity.[41;49;50;59] Analogous and consistent with the XRD and TGA results, the temperature of reduction should affect the electrical conductivity of these membranes. In-plane and out of plane conductivity of the GO membranes were measured after thermal treatment at temperatures of 60ºC, 180ºC, 225ºC and 250ºC. The out of plane conductivity provides a direct measure of the change in the interlayer spacing, the in plane conductivity on the other hand depends on both the inherent conductivity of the GO (and TrGO) sheets and the overlap between the sheets as these measurements are over length scale of 5 mm. Typically for such membranes the in-plane conductivity measurements are dominated by the charge transport characteristics of the GO (or TrGO) sheets.[12] As seen in Figure 3a, the in-plane conductivity increases by over 5 orders of magnitude between 60 ºC and 250 ºC. The charge hopping model given by equation 1[49;59-61] is used to fit the current-voltage data (the solid line in Figure 3a).

$$G = Y_o + G_o \exp\left(\frac{V}{aL}\right) \qquad \text{Equation 1}$$

Here V is the applied bias, L is the distance between the electrodes on the GO (TrGO) membrane over which the I-V measurements are conducted. a = KT/(0.18er); K is the Boltzmann's constant; T is the temperature of measurement; e is the absolute charge on the electron and r is the hopping distance. The parameter Go depends on, N, the density of states near the Fermi level and L, the localization length of the electronic wave functions. From the fit of equation 1, as seen in Figure 3b, the hopping distance reduces from ~ 5.2 nm at 60 ºC to 1.6 nm at 250 ºC. Similarly Go increases in going from 60 ºC to 250 ºC. The increase can be the combined effect on the localization length, L, and the density of states, N.

The out of plane conduction in these membranes is over their thickness which is on the order of a few microns, as seen in the inset of Figure 1a. This conduction (Figure 3c) shows a drastic increase as the temperature for thermal reduction is increased from 60 ºC to 250 ºC. The change can be modelled as being governed by two aspects: (a) Given the high electric field, tunneling is expected for the transport of the charge carriers across the sheets. (b) Direct contact between the sheets can be modelled as an ohmic resistance The combined equation fit to this model is:[62]

$$I = \frac{V}{R} + P_1 \times V^2 \times exp\left(-\frac{aE_c}{V}\right) \qquad \text{Equation 2}$$

Here E_c is the critical field for tunneling, a, is the length scale for the tunneling (this is considering that the term V/a is the effective electric field in the membrane) and R is the ohmic resistance of the film due to direct interlayer contact between the TrGO sheets in the membrane.

The parameters calculated from the fit of equation 2 to the data (the solid lines in Figure 3c) show that R reduces by over 6 orders of magnitude and aE_C by over 16 times (Figure 3d). The ohmic resistance can be considered to be dependent on the density of, direct inter-layer contacts between the TrGO sheets and the ordered regions in the TrGO sheets. As the thermal reduction temperature is increased the removal of the functional groups will lead to an increase in both these factors. The decrease in the path length due to the ~ 40% reduction in the interlayer spacing will be a minor effect, as the ohmic resistance scales linearly with the path length and hence cannot account for the observed decrease in this resistance. The decrease in aE_c is ~16 times and is much greater than the decrease in the inter-layer spacing as quantified by XRD. The initial drastic decrease in the aE_c between 60 ºC to 180 ºC may reflect the change in the dielectric constant of these membranes due to removal of water. Following this, the gradual decrease from 180 ºC to 250 ºC is the result of the reduction in the interlayer spacing.

The ability of the ions to diffuse across the graphene membrane (similar to the filtration and osmosis membranes) is affected both by the free volume available in the membrane and the presence of functional groups.[1-8;21;22] The diffusional characteristic of these membranes is studied by using them as a separator between two chambers, one filled with salt solution (100 mM $CaCl_2$ or 100mM NaCl) and other with de-ionized water (18 Mohm-cm resistivity). The increase in the

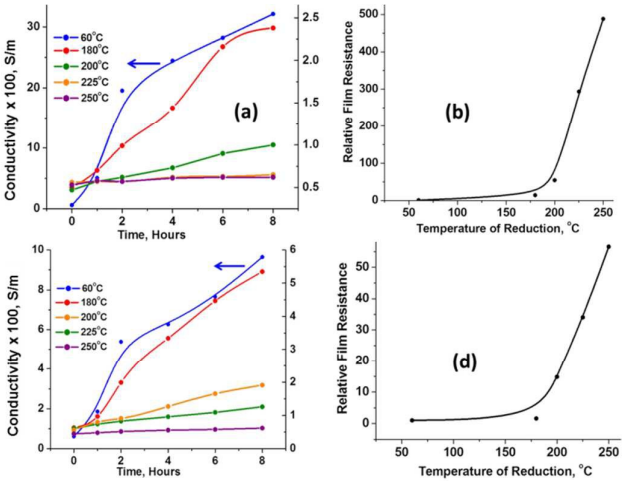

Figure 4. The evolution of the diffusional resistance of the TrGO membranes with temperature for salt solutions, NaCl and $CaCl_2$. (a) For diffusion from an 100mM NaCl solution, the diffusion rate decreases significantly on thermal reduction and the effect of temperature can be clearly observed. (b) Modelling the diffusion as being proportional to $t^{1/2}$ the diffusional resistance of the film is calculated and plotted. The resistance increases by over 2 orders of magnitude on reduction above the temperatures of 180°C. (c) A similar trend is observed for $CaCl_2$ where again a significant decrease in diffusion is observed. (d) The diffusion resistance again increases above 180°C, however the increase less drastic than that of NaCl.

conductivity of the di-ionized water resulting from the diffusion of the ions across the GO & TrGO membrane is monitored. The increase can be modelled (See ESI) to be proportional to $t^{1/2}$ (the elapsed time) and the diffusional resistance of the membrane. Figure 4a presents the observed increase in the conductivity of the de-ionised water (for 100 mM NaCl). From the fit (See ESI) the effective diffusional resistance for the Tr-GO membranes processed at different temperatures is calculated and the plot is shown in Figure 4b. We observe that the diffusional resistance of the membranes (relative to the 60°C membrane) increases rapidly above 180 ºC, in line with the rapid reduction in the inter-layer spacing and the removal of functional groups above those temperatures. A similar trend is observed for 100 mM $CaCl_2$, Figure 4c&d. For 100 mM CsCl diffusion behavior similar to NaCl is observed (see ESI).

For NaCl the change in resistance is over 500 times, significantly more drastic than $CaCl_2$ where it changes by ~60 times. This is due to the higher initial diffusion rate for the monovalent ion Na^+, which is consistent with its smaller size compared to Ca^{2+}. From the results it can be illustrated that GO films treated at 60 ºC have better selectivity towards the Na^+ and Ca^{2+} ions and this selectivity decreases predominantly due to loss of permeation of the Na^+ ions. For CsCl the change in resistance is similar to NaCl due the comparable radii of Na^+ and Cs^+.[63] The OH bond length in water molecule is ~ 0.96 °A.[64] Carbon nanotubes (CNT's) with water accessible pore diameter of 2 °A can transport water molecules as single files similar to biological channels and zeolites. [65-66] The channels in these GO films have also been used for microfluidic applications.[67] Fullerene, C_{60}, with a spherical diameter of 3.7 °A can encapsulate single water molecules. [68] The hydrated radii of Na^+ and Ca^{2+} ions is ~3.6 °A and 4.1 °A,[63] and is much larger than the water molecule and comparable to the average interlayer spacing of 4.6 °A for the TrGO membranes reduced at 250 °C. Considering this along with the observation that the inter-layer spacing has a broad distribution in the TrGO membranes reduced at 250 °C (& also 225 °C & 300 °C), the diffusion of the ions across these membranes is hindered. The water molecules however due to their much smaller size are able to access the TrGO membranes.

Conclusions

The ability to control the diffusional characteristics of the GO membrane by thermal treatment and the temperature of exposure illustrated above is a simple method to tailor their properties. Further this can also be expanded to include the effect on diffusion of small organic molecules and also gas permeation. The key factor is the spacing between the TrGO sheets in the membrane. This spacing is dependent on the degree of reduction of the GO sheets and can be controlled by the temperature of reduction. Two distinct regions exist, one below 180°C and the other above 225°C. The transition between the two regions provides an ability to control the spacing between the two extremes of ~ 7°A and 4.6°A. While the spacing affects the diffusion characteristics of the membrane, it also has a similar effect on the electrical conduction properties. The combined control over the electrical conductivity and diffusion characteristic is important for other potential applications such as supercapacitors, electrochemical sensors, capacitive desalination and using them as protective coatings and fillers in composites.

Acknowledgements

This work was supported by the Saudi Cultural Bureau and Taif University, University of Waterloo, Canada Foundation for Innovation, Ontario Research Fund and NSERC Canada.

Notes and references

1 M. Hu, B. X. Mi, *Environ. Sci. Technol.* 2013, **47,** 3715.
2 D. E. Jiang, V. R. Cooper, S. Dai, *Nano Lett.* 2009, **9** 4019.
3 R. K. Joshi, P. Carbone, F. C. Wang, V. G. Kravets, Y. Su, I. V. Grigorieva, H. A. Wu, A. K. Geim, R. R. Nair, *Science* 2014, **343,** 752.
4 H. W. Kim, H. W. Yoon, S. M. Yoon, B. M. Yoo, B. K. Ahn, Y. H. Cho, H. J. Shin, H. Yang, U. Paik, S. Kwon, J. Y. Choi, H. B. Park, *Science* 2013, **342,** 91.
5 W. Guo, C. Cheng, Y. Wu, Y. Jiang, J. Gao, D. Li, L. Jiang, *Adv. Mater.* 2013, **25,** 6064.
6 K. Sint, B. Wang, P. Kral, *J. Am. Chem. Soc.* 2008, **130**, 16448.
7 P. Z. Sun, M. Zhu, K. L. Wang, M. L. Zhong, J. Q. Wei, D. H. Wu, Z. P. Xu, H. W. Zhu, *Acs Nano* 2013, **7**, 428.
8 A.R. Koltonow, J. Huang, *Science* 2016, **351**, 6280.

9 S. Salgado, L. Pu, V. Maheshwari, *J. Phys. Chem. C* 2012, **116,** 12124.
10 M. Pumera, *Chem. Soc. Rev.* 2010, **39**, 4146.
11 Y. T. Kim, J. H. Han, B. H. Hong, Y. U. Kwon, *Adv. Mater.* 2010, 22, 515.
12 C. X. Guo, X. T. Zheng, Z. S. Lu, X. W. Lou, C. M. Li, *Adv. Mater.* 2010, **22**, 5164.
13 C. Liu, S. Alwarappan, Z. F. Chen, X. X. Kong, C. Z. Li, *Biosens. Bioelectron.* 2010, **25,** 1829.
14 Z. S. Wu, A. Winter, L. Chen, Y. Sun, A. Turchanin, X. L. Feng, K. Mullen, *Adv. Mater.* 2012, **24,** 5130.
15 Y. Ohno, K. Maehashi, Y. Yamashiro, K. Matsumoto, *Nano Lett.* 2009, **9**, 3318.
16 Z. G. Cheng, Q. Li, Z. J. Li, Q. Y. Zhou, Y. Fang, *Nano Lett.* 2010, **10**, 1864.
17 M. D. Stoller, S. J. Park, Y. W. Zhu, J. H. An, R. S. Ruoff, *Nano Lett.* 2008, **8,** 3498.
18 Y. Y. Li, Z. S. Li, P. K. Shen, *Adv. Mater.* 2013, **25**, 2474.
19 Y. Wang, Z. Q. Shi, Y. Huang, Y. F. Ma, C. Y. Wang, M. M. Chen, Y. S. Chen, *J. Phys. Chem. C* 2009, **113**, 13103.
20 Y. P. Zhang, H. B. Li, L. K. Pan, T. Lu, Z. Sun, *J. Electroanal. Chem.* 2009, **634**, 68.
21 J. S. Bunch, S. S. Verbridge, J. S. Alden, A. M. van der Zande, J. M. Parpia, H. G. Craighead, P. L. Mceuen, *Nano Lett.* 2008, **8**, 2458.
22 O. Leenaerts, B. Partoens, F. M. Peeters, *Appl. Phys. Lett.* 2008, **93**, 193107.
23 D. Menshykau, I. Streeter, R. G. Compton, *J. Phys. Chem. C* 2008, **112**, 14428.
24 C. Punckt, M. A. Pope, J. Liu, Y. H. Lin, I. A. Aksay, *Electroanalysis* 2010, **22**, 2834.
25 C. Punckt, M. A. Pope, I. A. Aksay, *J. Phys. Chem. C* 2014, **118,** 22635.
26 D.A. Dikin, S. Stankovich, E.J. Zimney, R.D. Piner, G.H.B. Dommett, G. Evmenenko, S.T. Nguyen, R.S. Ruoff, *Nature* 2007, **448,** 457.
27 S. Park, K.S. Lee, G. Bozoklu, W. Cai, S.T. Nguyen, R.S. Ruoff, *ACS Nano* 2008, **2,** 572.
28 O.C. Compton, S.W. Cranford, K.W. Putz, Z. An, L.C. Brinson, M.J. Buehler, S.T. Nguyen, *ACS Nano* 2012, **6,** 2008.
29 Z. Li, I.A. Kinloch, R.J. Young, K.S. Novoselov, G. Anagnostopoulos, J. Parthenios, C. Galiotis, K. Papagelis, C.Y. Lu, L. Britnell, *ACS Nano* 2015, **9,** 3917.
30 Y. Lan, H. Liu, X. Cao, S. Zhao, K. Dai, X. Yan, G. Zheng, C. Liu, C. Shen, Z. Guo, *Polymer* 2016, **97,** 11.
31 B. Jiang, L. Zhao, J. Guo, X. Yan, Y. Hunag, Z. Guo, *J. Nanopart. Res.* 2016, **18,** 145.
32 H. Liu, J. Gao, W. Huang, K. Dai, G. Zheng, C. Liu, C. Shen, X. Yan, J. Guo, Z. Guo, *Nanoscale* 2016 DOI 10.1039/C6NR02216B
33 L. Shao, X. Chang, Y. Zhang, Y. Huang, Y. Yao, Z. Guo, *Appl. Surf. Sci.* 2013, **280,** 989.
34 L. Shao, S. Quan, Y. Liu, Z. Guo, Z. Wang, *Mater. Lett.* 2013, **107,** 307.
35 Z. L. Wang, D. Xu, Y. Huang, Z. Wu, L. M. Wang, X. B. Zhang, *Chem. Commun.* 2012, **48**, 976.
36 W.S. Hummers, R.E. Offeman, *J. Am. Chem. Soc.* 1958, **80**, 1339.
37 N. I. Kovtyukhova, P. J. Ollivier, B. R. Martin, T. E. Mallouk, S. A. Chizhik, E. V. Buzaneva, A. D. Gorchinskiy, *Chem. Mater.* 1999, **11,** 771.
38 H. Chen, M. B. Muller, K. J. Gilmore, G. G. Wallace, D. Li, *Adv. Mater.* 2008, **20,** 3557.
39 G. Eda, G. Fanchini, M. Chhowalla, *Nature Nanotech.* 2008, **3,** 270.
40 C. Punckt, M. A. Pope, I. A. Aksay, *J. Phys. Chem. C* 2013, **117,** 16076.
41 C. Punckt, F. Muckel, S. Wolff, I. A. Aksay, C. A. Chavarin, G. Bacher, W. Mertin, *Appl. Phys. Lett.* 2013, **102**, 023114.
42 A. Lerf, H. Y. He, M. Forster, J. Klinowski, *J. Phys. Chem. B* 1998, **102,** 4477.
43 M. J. McAllister, J. L. Li, D. H. Adamson, H. C. Schniepp, A. A. Abdala, J. Liu, M. Herrera-Alonso, D. L. Milius, R. Car, R. K. Prud'homme, I. A. Aksay, *Chem. Mater.* 2007, **19,** 4396.
44 S. Stankovich, D. A. Dikin, R. D. Piner, K. A. Kohlhaas, A. Kleinhammes, Y. Jia, Y. Wu, S. T. Nguyen, R. S. Ruoff, *Carbon* 2007, **45,** 1558.
45 X. W. Wang, Z. P. Xiong, Z. Liu, T. Zhang, *Adv. Mater.* 2015, **27,** 1370.
46 C. Zhang, D. M. Dabbs, L. M. Liu, I. A. Aksay, R. Car, A. Selloni, *J. Phys. Chem. C* 2015, **119**, 18167.
47 J. G. Radich, P. V. Kamat, *Acs Nano* 2013, **7,** 5546.
48 S. Pei, H.M. Cheng, *Carbon* 2012, **50**, 3210.
49 A. B. Kaiser, C. Gomez-Navarro, R. S. Sundaram, M. Burghard, K. Kern, *Nano Lett.* 2009, **9,** 1787.
50 I. Jung, D. A. Dikin, R. D. Piner, R. S. Ruoff, *Nano Lett.* 2008, **8**, 4283.
51 M. A. Pope, C. Punckt, I. A. Aksay, *J. Phys. Chem. C* 2011, **115**, 20326.
52 R. Narayanan, H. Yamada, M. Karakaya, R. Podila, A. M. Rao, P. R. Bandaru, *Nano Lett.* 2015, **15**, 3067.
53 L. F. Lai, H. P. Yang, L. Wang, B. K. Teh, J. Q. Zhong, H. Chou, L. W. Chen, W. Chen, Z. X. Shen, R. S. Ruoff, J. Y. Lin, *Acs Nano* 2012, **6**, 5941.
54 D. T. L. Galhena, B. C. Bayer, S. Hofmann, G. A. J. Amaratunga, *Acs Nano* 2016, **10**, 747.
55 Z. S. Wu, K. Parvez, A. Winter, H. Vieker, X. J. Liu, S. Han, A. Turchanin, X. L. Feng, K. Mullen, *Adv. Mater.* 2014, **26**, 4552.
56 M. Q. Zhao, Y. F. Zhou, M. L. Bruening, D. E. Bergbreiter, R. M. Crooks, *Langmuir* 1997, **13**, 1388.
57 S. V. Morozov, K. S. Novoselov, M. I. Katsnelson, F. Schedin, D. C. Elias, J. A. Jaszczak, A. K. Geim, *Phys. Rev. Lett.* 2008, **100,** 016602.
58 K. S. Novoselov, A. K. Geim, S. V. Morozov, D. Jiang, Y. Zhang, S. V. Dubonos, I. V. Grigorieva, A. A. Firsov, *Science* 2004, **306,** 666.
59 C. Gomez-Navarro, R. T. Weitz, A. M. Bittner, M. Scolari, A. Mews, M. Burghard, K. Kern, *Nano Lett.* 2007, **7**, 3499.
60 M. M. Fogler, S. Teber, B. I. Shklovskii, *Phys. Rev. B* 2004, **69**, 035413.
61 M. Pollak, I. Riess, *J. Phys. C-Solid State Phys.* 1976, **9**, 2339.
62 V. Maheshwari, R. F. Saraf, *Science* 2006, **312**, 1501.
63 E.R. Nightingale, *J. Phys. Chem.* 1959, **63,** 1381.
64 D. Hankins, J.W. Moskowit, F.H. Stillinger, *J. Chem. Phys.* 1970, **53,** 4544.
65 A. Berezhkovskii, G. Hummer, *Phys. Rev. Lett.* 2002, **89,** 064503.
66 P. Agre, D. Kozono, *FEBS Letters* 2003, **555,** 72.
67 K. Raidongia, J. Huang, *J. Am. Chem. Soc.* 2012, **134,** 16528.
68 K. Kurotobi, Y. Murata, *Science* 2011, **333,** 613.

Inter-layer spacing in reduced graphene-oxide membranes which modulates their ion-diffusion, electrical and electrochemical characteristics is controlled by temperature of thermal reduction.